Powder Metallurgy High Nitrogen Stainless Steel

F. S. Biancaniello, R. D. Jiggetts, R. E. Ricker and S. D. Ridder

Metallurgy Division, National Institute of Standards and Technology
Gaithersburg, MD 20899, USA

Keywords: austenitic stainless steel, duplex stainless steel, high nitrogen steel, improved structural and corrosion properties, modeling, nitrogen solubility, phase stability, pitting corrosion, powder processing.

Abstract High Nitrogen Stainless Steels (HNSS) are a class of materials that possess a unique combination of outstanding strength, ductility, and corrosion properties. In this paper we report on the advantages of producing these materials via inert gas atomization and HIP consolidation. The high homogeneity and microstructural refinement of Powder Metallurgy (PM) processing was employed to produce a series of HNSS alloys with enhanced nitrogen solubility that possess mechanical and corrosion properties that are as good as or better than previously reported results. The high nitrogen solubility was achieved using alloy chemistry modifications and atmospheric nitrogen pressures. A model was generated by utilizing our own database of measured chemistry and property data that predicts nitrogen content and phase stability. Microstructure, mechanical properties, and corrosion properties are presented as a function of alloy content.

Introduction Early research on nitrogen-containing iron alloys was first reported at the Carnegie Institute in 1912 [1]. In the 1920's and 1930's, additional research was conducted in Europe, primarily in Germany, and to a lesser degree in the United States [2]. Later in the 1970's, Armco developed a series of nitrogen containing steel alloys (the Nitronic® alloys)*, with specific alloys designed for either high strength, wear resistance or improved corrosion properties [3]. The last 10 to 15 years have witnessed a dramatic increase in high nitrogen steel (HNS) research as evidenced by four previous international conferences on HNS [4-7] and currently in 1998, the fifth international HNS is being conducted in Helsinki and Stockholm. Despite the outstanding properties that a growing number of researchers have attributed to HNS [2, 8], several factors can limit the potential of these alloys. These factors include: a) the formation of brittle, stable nitrides and inter-metallics which can precipitate during the slow cooling encountered during ingot casting, b) other casting defects such as macrosegregation which can render these highly alloyed materials unworkable by conventional wrought processing techniques [9, 10], and c) the difficulty in producing predictable nitrogen levels during both conventional and pressurized casting methods [9, 11, 12].

Prior research [11, 13] has shown that many of the problems can be overcome by melting HNSS under a nitrogen atmosphere, atomizing with N_2 gas and consolidating with a Hot Isostatic Press (HIP). The beneficial effects of nitrogen on the properties of HNSS have been reviewed in previous research studies [8, 11]. In summary, the yield strength (YS), ultimate tensile strength (UTS) Charpy V-notch Impact Energy (CVN), corrosion and wear properties all increase with increasing nitrogen content [8, 11]. Nitrogen promotes the stability of the austenite phase (no martensite formation during cold work) [14], and improves resistance to all types of corrosion [15]. The

*References to commercial trademarks are for identification purposes only and in no way constitute endorsement or evaluation of the relative merits of these products.

benefits of nitrogen additions are reinforced by the microstructural refinements, enhanced chemical homogeneity and increased solubility of constituents which convey from PM rapid solidification processing (RSP). RSP and HIP also provide the opportunity for near-net-shape fabrication of the alloys, minimizing machining time and scrap. The alloys described in this study were prepared by N_2 gas atomization in the NIST Supersonic Inert Gas Metal Atomizer (SIGMA) followed by HIP consolidation [13] and hot extrusion. The goal of this research was to produce an HNSS alloy with mechanical properties to exceed a UTS of 1050 MPa, an elongation of 50 %, and a CVN of 120 J, and the pitting corrosion resistance was designed to exceed the performance of implant grade 316L stainless.

Experiments To achieve these goals, a multi-variable regression analysis was performed on compositional and property data generated from 60 prior atomization runs. This resulted in a set of coefficients that represented the sensitivity of each constituent on nitrogen solubility, mechanical properties, and corrosion resistance. In addition, prior work by Reichsteiner [16] provided coefficients that could be used to determine whether an alloy would contain detrimental ferrite within the austenite matrix phase. This predictive model was then encoded in a spreadsheet format that permitted efficient evaluation of alloy compositions prior to running the costly atomization trials. The performance goals set for these alloys narrowed the number of alloy constituents and range of compositions. The minimum N mass fraction was set at 0.8 % to ensure high strength and austenite stability but was not allowed to exceed 0.95 % to preclude the formation of stable nitrides (i.e. Cr_2N). The Cr mass fraction was set relatively high (28 % to 30 %) to ensure a high nitrogen level and the Mo mass fraction was set at 2 % to help improve corrosion properties. Higher values were not used because of cost and the tendency of Mo to form the intermetallic σ phase. Mn concentration was limited to 15 % to minimize its detrimental effects on corrosion properties. Ideally, for improved corrosion properties, the mass fraction of Mn should not exceed 10 %, however, this requirement was relaxed in this series of alloys in order to reach minimum 0.8 % N solubility [8]. Finally, Ni, although high in cost and detrimental to N solubility, was maintained above 12 % to insure austenite stability.

Results and Discussion Table 1 shows measured compositions of the HNSS alloys produced in this study. The alloys numbered *NSS.082* to *NSS.087* are the experimental alloys that resulted from using the predictive model with the performance and composition criteria mentioned previously. Alloy *NSS.057* (from a prior study [13]) is included for comparison purposes and represents a typical HNSS alloy where reduced Cr, Mn, and N result in a duplex microstructure. Duplex stainless steels consist of a mixture of austenite and ferrite within the matrix as seen in Fig. 1. Table 2 shows N content predicted by regression analysis (N_R) and measured (N_M), hardness, strength, elongation, strain-hardening exponent (*n*), and CVN for each of the alloys shown in Table 1. Measurements were made using methods described in ASTM E8 for UTS, YS, and elongation, ASTM E646 was followed to calculate *n* values, and ASTM E23 was followed to calculate impact energy [17]. The indicated property values are an average of two test samples where the evaluated uncertainties (2σ) for UTS and YS values are ±17 MPa, ±1.3 % for elongation

Table 1 Alloy Compositions (mass fraction %).

Alloy #	Fe	Cr	Ni	Mn	Mo	N	Si	O	C	S
NSS.057	62.59	24.97	4.84	4.06	3.00	0.50	0.00	0.019	0.016	<.003
NSS.082	40.79	29.82	13.93	11.99	1.94	0.97	0.48	0.059	0.017	0.002
NSS.083	42.56	29.90	13.91	10.29	1.95	0.94	0.37	0.055	0.021	0.003
NSS.084	39.27	27.42	14.94	15.07	1.93	0.84	0.46	0.045	0.019	0.003
NSS.085	43.81	29.65	15.13	8.03	1.96	0.86	0.50	0.046	0.014	0.003
NSS.086	46.33	29.35	15.02	5.96	1.94	0.83	0.51	0.044	0.016	0.003
NSS.087	45.29	29.49	12.85	9.00	1.92	0.88	0.50	0.042	0.020	0.004

Table 2 Alloy Properties

Alloy #	N_R (%)	N_M (%)	hardness (HV_{1000})	YS (MPa)	UTS (MPa)	% elong.	*n*	CVN (J)
NSS.057	0.51	0.50	312	602	956	32.30	0.181	25
NSS.082	0.84	0.97	303	642	1096	55.70	0.214	69
NSS.083	0.79	0.94	298	635	1089	59.35	0.218	115
NSS.084	0.81	0.84	293	565	1034	57.85	0.231	126
NSS.085	0.73	0.86	296	609	1066	57.80	0.221	140
NSS.086	0.69	0.83	275	591	1066	53.90	0.225	132
NSS.087	0.77	0.88	300	642	1100	53.10	0.213	129

values, ±0.003 for *n* values, and ±4 J for impact energy. Volume fraction austenite was found to be in excess of 0.99 for all the alloys listed (as determined by x-ray diffraction analysis and optical metallography) except *NSS.057* where volume fraction austenite was found to be 0.67.

Prior studies by the authors [13] and others [14, 18] have found it necessary to solution treat and water quench HNSS alloys to eliminate the previously mentioned Cr_2N and σ phases. Fig. 1 shows micrographs of alloy *NSS.057* both before and after this solution treatment. The darkly etched intermetallic precipitates within the duplex matrix are clearly visible in Fig. 1a. This same alloy after solution treatment to dissolve these inclusions is shown in Fig. 1b.

Although solution treatment is effective in eliminating these phases, the duplex matrix was still a source of some concern. The ferrite phase is known to affect certain mechanical properties. Ferrite can cleave and fail catastrophically, austenite can not cleave, it fails by a ductile mode [10, 19]. Ferrite also reduces corrosion resistance, and the ferrite crystal structure has a much lower N solubility than austenite. Therefore, in this new set of alloys the chemistry was adjusted with an intent of producing an 100 % austenite material. The photomicrograph shown in Fig. 2 (*NSS.085* after HIP consolidation) is typical of the austenitic alloys in this study. Fine equiaxed grains (≈25 μm) of austenite are accompanied by small precipitates of manganese silicate amounting to less than 1 % of the volume. Fig. 3 is a typical x-ray diffraction pattern produced by these alloys. No evidence of secondary phases was seen in any of these newer alloys either before or after HIP consolidation. The relatively high CVN's (exceeding 100 J in all but alloy *NSS.082*) are further

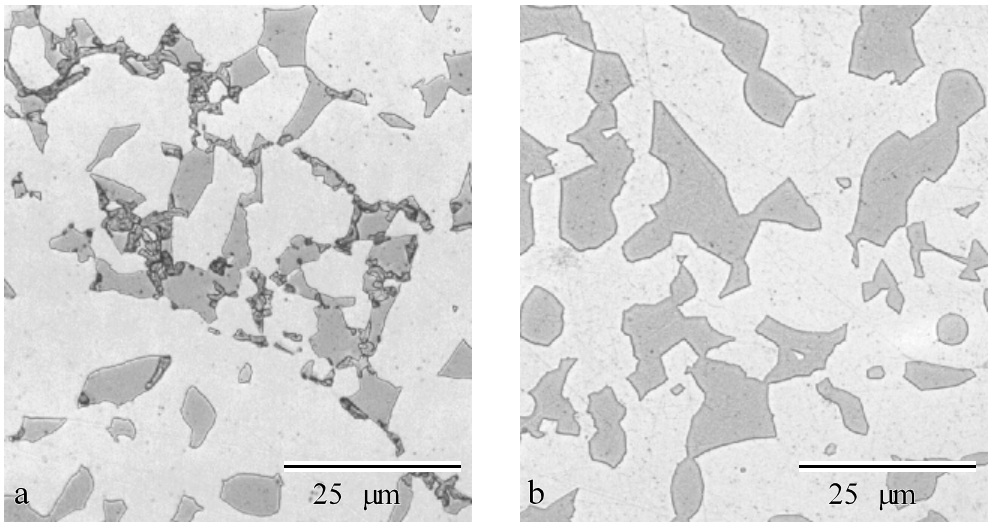

Figure 1 Micrographs of NSS.057 showing duplex structure. **a**) As HIPped showing Cr_2N and σ phase inclusions. **b**) HIPped and solution treated.

evidence of the elimination of these undesirable second phases. These new austenitic HNSS chemistries reduce production costs by eliminating costly solution treatments and allow fabrication of thicker sections (quench sensitivity in the previous alloys limited specimen thickness). It is also possible that the "cleaner" microstructure could result in improved corrosion and mechanical properties.

The data in Table 2 demonstrate that in general, as the N content is increased, mechanical properties are improved. As the N mass fraction varies from 0.83 % to 0.97 % the Vickers microhardness varies from 280 HV_{1000} to 303 HV_{1000}, the YS varies from 565 MPa to 642 MPa, and UTS varies from 1034 MPa to 1100 MPa. The microhardness and YS data are plotted in Figs. 4 and 5 where error bars indicate the 2σ uncertainty in the measured values (±8 HV_{1000} and ±17 MPa respectively).

The increased hardness conferred by the increased nitrogen content and high *n* values are expected to result in an improvement in wear resistance. Preliminary evaluation shows the coefficient of friction of these alloys, measured in dry pin-on-disk testing (HNSS against HNSS), to fall in the range $\mu = 0.5$ to 0.6, which is similar to commercial steels. A tribological investigation for these alloys is under way and will be reported on in a future publication.

The relative corrosion resistance of these alloys was evaluated by conducting electrochemical polarization experiments. In these experiments, the relative corrosivity of the environment required to cause pitting of the different alloys was quantitatively assessed by increasing the potential of the sample with respect to this reference reaction in a slow and continuous manner until pitting occurred. With this technique, the onset of pitting can be detected by relatively large increases in current which were then verified with optical microscopy. Fig. 6 is a plot of polarization currents as a function of the potential of the samples with respect to an electrochemical reference reaction in a solution commonly used to evaluate the corrosion resistance of alloys for orthopedic implants (Hanks solution at 37 °C) [20]. From this figure it can be seen that pitting did not occur in any of the alloys in this study until the potential was 600 mV higher than that required to cause pitting of orthopedic implant grade 316L. This means that these alloys are significantly more resistant to pitting in this environment than 316L and that a significantly higher oxidizing potential (oxidizer content) would be required to cause pitting of this alloys as compared to 316L. In fact, these

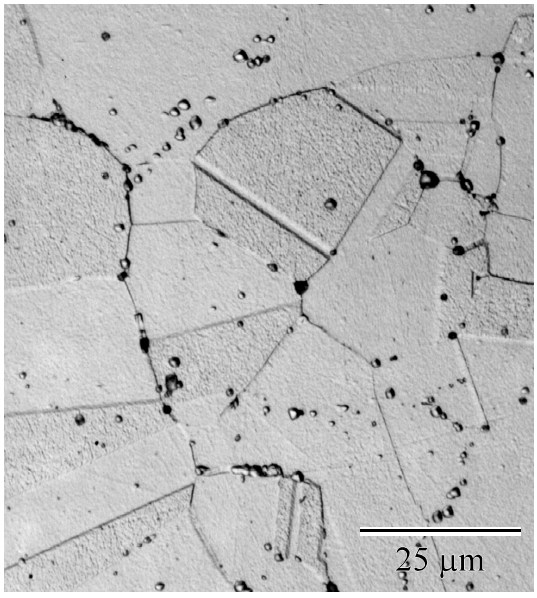

Figure 2 Micrograph of consolidated HNSS showing a fully dense, equiaxed grain structure.

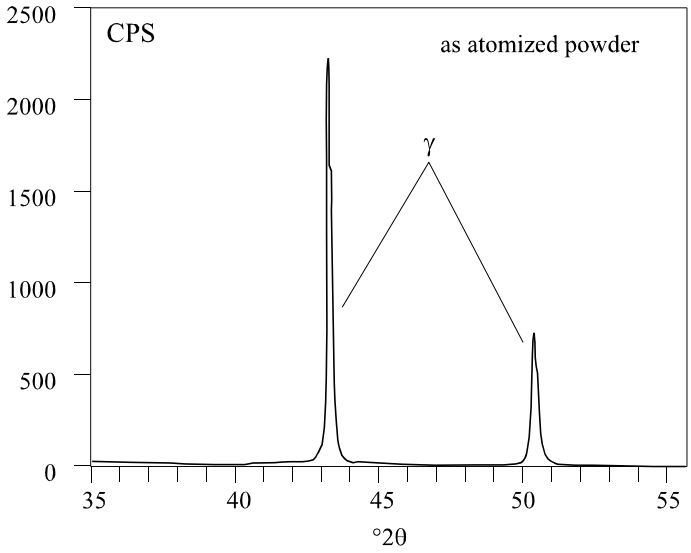

Figure 3 X-ray diffraction data from single phase austenite atomized powder.

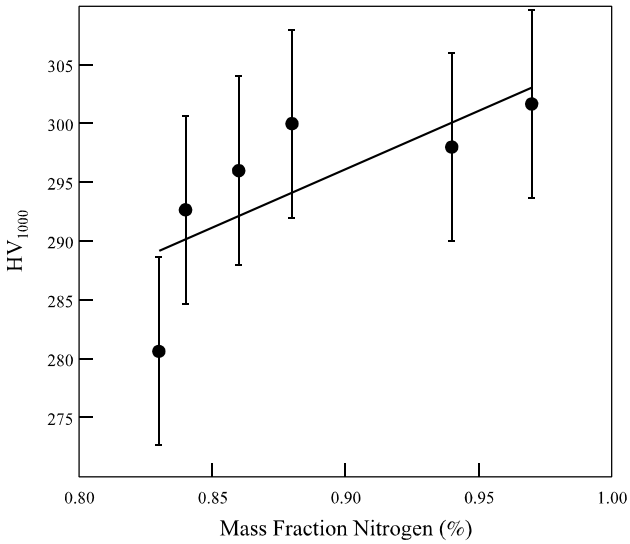

Figure 4 Plot of hardness vs. nitrogen content data from Table 2.

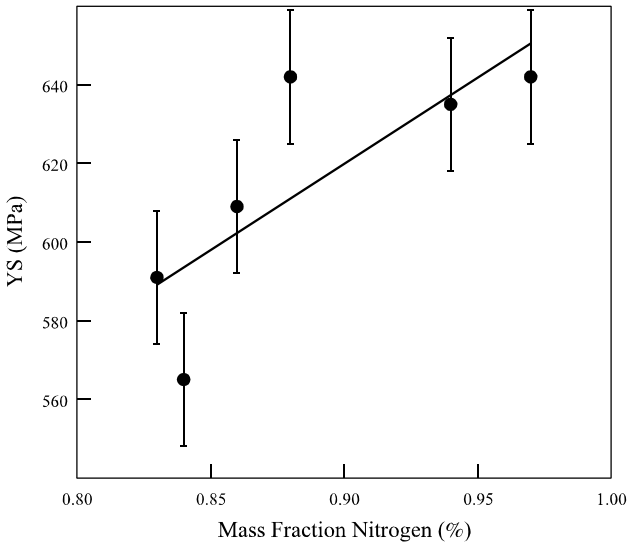

Figure 5 Plot of YS vs. nitrogen content data from Table 2.

measurements indicate that oxidizing species in the environment must provide 58 kJ per equivalent more energy to cause pitting of these alloys compared to 316L. While these alloys have a significantly greater resistance to pitting corrosion than 316L, the pitting resistance of these alloys was not as great as expected based on earlier work [13]. As a result, additional research into the corrosion behavior of these alloys is underway that should illuminate the origins of this behavior and enable optimization of the corrosion resistance of these alloys.

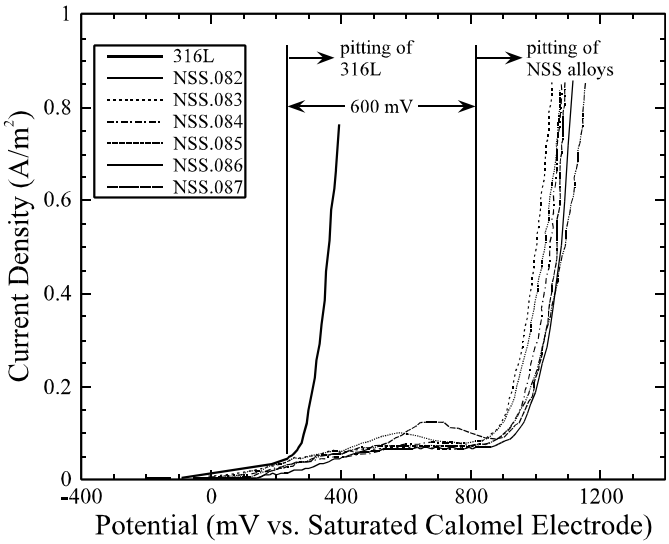

Figure 6 Polarization current vs. potential for HNSS alloys.

Conclusions An alloy chemistry modeling tool was used that can accurately predict the N solubility in austenitic and duplex stainless steels. Targeted mechanical and corrosion properties were achieved in a series of alloys designed using this modeling tool. The mechanical property data presented for these HIP consolidated powder metallurgy HNSS alloys, in particular, the high ductility (> 50% elongation), relatively high *n* values (≈0.2), and good impact properties of these alloys, are evidence of resistance to brittle failure and expected good wear properties. Electrochemical tests demonstrated significantly improved pitting resistance relative to 316L and similar alloys in a physiological solution. In addition intermetallic precipitates were completely eliminated, improving mechanical and corrosion properties while reducing processing steps.

Acknowledgments The authors wish to thank R. L. Parke, P. A. Boyer, L. C. Smith, J. L. Fink, R. D. Schmidt, M. E. Williams, and J. R. Manning for their invaluable assistance in various aspects of this study. In addition we wish to recognize the valuable collaboration with J. J. Conway at Crucible Compaction Metal and G. O. Rhodes at Crucible Research Corporation.

References

[1] J.H. Andrew, in *Carnegie Scholarship Memoirs*, **3**, (1912), p. 236.
[2] H.K. Feichtinger and X. Zheng, Powder Metall. Int. **36**, 7 (1990). p. 7.
[3] *Development of the Stainless Steels*, Armco Inc., Middletown, Ohio (1983)
[4] *High Nitrogen Steels*, Inst. Met., London (1989)
[5] *High Nitrogen Steels*, Stahl & Eisen, Dusseldorf (1993)
[6] *High Nitrogen Steels*, Inst. Met. Phys., Kiev (1993)
[7] *High Nitrogen Steels*, ISIJ Int., Tokyo (1996)
[8] M.O. Speidel, Inst. Met., in *High Nitrogen Steels*, Inst. Met., London (1989), p. 92.
[9] V.G. Gavriljuk, in *High Nitrogen Steels*, ISIJ Int. 36, Tokyo (1996), p. 738.
[10] *Metals Handbook Ninth Edition*, ASM, 7, (1984), p. 439.
[11] R.P. Reed, J. Met. **41**, 3 (1989), p. 16.
[12] G.O. Rhodes and J.J. Conway, J. Met. **48**, 4 (1996), p. 28.
[13] F.S. Biancaniello et. al., in *Advanced Particulate Materials & Processes 1997*, MPIF (1997), p. 309.
[14] A. Soussan et. al., in *High Nitrogen Steels*, Stahl & Eisen, Dusseldorf (1993), p. 67.
[15] H.J. Grabke, in *High Nitrogen Steels*, ISIJ Int. 36, Tokyo (1996), p. 777.
[16] A. Rechsteiner and M.O. Speidel, Assoc. In *New Methods for the Production of High Nitrogen Stainless Steels*, It. di Met., Milan (1993), p. 2107.
[17] *Annual Book of ASTM Standards*, ASTM, 3.01, (1997).
[18] G.O. Rhodes et. al., in *Advanced Particulate Materials & Processes 1997*, MPIF (1997), p. 295.
[19] N.E. Dowling, *Mechanical Behavior of Materials: Engineering Methods for Deformation, Fracture, and Fatigue*, Prentice Hall, Englewood Cliffs, NJ, (1993), p. 309.
[20] A.T. Kuhn et. al., in *The Use of Synthetic Environments for Corrosion Testing*, ASTM STP 970, ASTM, (1988), p. 79.